Heliyon xxx (xxxx) xxx

Contents lists available at ScienceDirect

Heliyon

journal homepage: www.cell.com/heliyon

Research article

Synthesis, characterization, *in silico,* and *in vitro* biological screening of coordination compounds with 1,2,4-triazine based biocompatible ligands and selected 3d-metal ions

Rugmini Ammal P [a], Anupama R. Prasad [b], Abraham Joseph [b,*]

[a] *Department of Chemistry, Zamorin's Guruvayurappan College, Calicut, India*
[b] *Department of Chemistry, University of Calicut, Kerala, India*

ARTICLE INFO

Keywords:
Inorganic chemistry
MHMMT
α-amylase
Molecular docking
Geometry

ABSTRACT

A bidentate Schiff base ligand, MHMMT, obtained from 1,2,4-triazine derivative and 4-hydroxy-3-methoxy benzaldehyde and its Fe(III), Co(II), Ni(II), Cu(II), and Zn(II) complexes were synthesised in ethanolic media and characterized by various analytical techniques like elemental analyses, magnetic susceptibility measurements, FTIR, UV-VIS, proton NMR, ESR, spectroscopic and thermogravimetric studies. Various geometries like a tetrahedral for Co(II) and Zn(II) complexes, an octahedral for Fe(III) and Ni(II) complexes, and square planar for Cu(II) complex has been assigned. For all metals complexes except Co(II), a 2:1 ligand to metal ratio is observed, while Co(II) complex has a 1:1 ratio. In accordance with the probable activity spectra of substances as obtained from PASS analysis, *in vitro* α-amylase inhibition studies by starch-iodine method for ligand and complexes except that of Fe(III) and anticancer screening against human breast cancer cell lines MCF-7 using MTT assay for Fe(III) complex were conducted. The tested compounds were found to be good α-amylase inhibitors, characteristically similar to most of the antidiabetic drugs. Among the compounds, Cu(II) complex exhibited the highest α-amylase inhibitory activity. Furthermore, ligand and complexes were also exposed to *in vitro* antimicrobial activities, drug-likeness, bioactivity score prediction by Molinspiration software. Molecular docking analysis of selected compounds on α-amylase and VEGFR-2 kinase were carried out for confirming the experimental observations.

1. Introduction

Coordination compounds with its promising specialties and applications became a centre of attraction in diverse fields of biological and chemical researches [1]. After extensive research for decades, a structure-activity relationship was established for these compounds and this paved the way for designing various N, S, O donor heterocycles as scaffolds for talented compounds with fantabulous properties. The properties like versatile coordination modes, diverse applications in various fields, corrosion inhibition, etc. made them a topic of increasing interest in the current research scenario. During recent years, investigations on Schiff bases possessing N, S, O heterocycles like 1,2,4-triazines became a hot spot in the research arena [2, 3, 4, 5]. It was suggested that the azomethine linkage, as well as additional donor sites in 1,2,4-triazine moieties, make them more versatile and flexible with biological, pharmacological, and medicinal properties [6, 7]. Transition metal complexes of Schiff bases derived from amino-substituted 1,2,4-triazines and various carbonyl compounds have become increasingly important due to their auspicious uses [8, 9, 10]. Many of these Schiff bases as well as their metal complexes provided a rich platform for various interesting biological effects like antibacterial, antifungal, anticancer, anti-inflammatory, antimalarial, and various other effects.

Literature has revealed an umpteen number of investigations on complex formation and biological studies on various 1,2,4-triazine based Schiff bases and their transition metal complexes. Owing to the elucidation of interdisciplinary research between chemistry and biology as a land mark in complex chemistry, many workers in this field focused their studies towards the biological activities along with molecular modelling.

By considering the above facts and as a continuation of our interest on transition metal complexes and exploring their biological properties, herein we present the synthesis, characterization and *in silico* and *in vitro* biological screening for antifungal, anticancer and antidiabetic activities as well as molecular docking studies of 4-[(4-hydroxy-3-methoxybenzylidene)amino]-6-methyl-3-thioxo-3,4-dihydro-1,2,4-triazin-

* Corresponding author.
E-mail address: drabrahamj@gmail.com (A. Joseph).

https://doi.org/10.1016/j.heliyon.2020.e05144
Received 8 July 2020; Received in revised form 11 August 2020; Accepted 29 September 2020

5(2*H*)-one(MHMMT) and some of its selected transition metal complexes in this paper.

2. Experimental

2.1. Materials and methods

The reagents employed for the present work were of analar grade obtained from commercial sources and used without further purifications. Percentage of carbon, hydrogen, nitrogen, and Sulphur in the ligand as well as complexes were determined using a CHNS analyser (Elementar Vario EL III Model). The percentage of metal in the complexes was determined by standard procedures [11]. The magnetic susceptibility studies were carried out in a Gouy balance (Sherwood Scientific Cambridge, UK) at room temperature using $Hg[Co(SCN)_4]$ as calibrant. The Infra red spectra of the ligand as well as complexes were conducted using KBr pellet method on a JASCO FTIR-4100 instrument in 4000-400 cm^{-1} region. The proton NMR spectra of ligand as well as its diamagnetic zinc complex was taken in solution front using DMSO 6d as the solvent in Bruker Avance III 400 MHz NMR instrument using TMS as the internal standard. The X band EPR spectra of the copper complex were recorded at 77 K in DMF with a JES-FA200 ESR spectrometer using Mn^{2+} as a marker. The electronic spectra of the ligand as well as paramagnetic metal complexes were recorded using JASCO-V-550 spectrophotometer both in diffused reflectance mode and in solution form.

2.2. Synthesis of 4-amino-3-mercapto-6-methyl-1,2,4-triazine-4H-5-one (AMMOT) and Schiff base MHMMT

1,2,4-triazine derivative, 4-amino-3-mercapto-6-methyl-1,2,4-triazine-4H-5-one (AMMOT) was synthesized in two steps. In the first step, to a mixture of 50 mL of hydrazine hydrate and 150 mL of water, about 0.2 mol of carbon disulphide (CS_2) was added dropwise over about an hour maintaining the temperature below 15 °C with constant and vigorous stirring. After the completion of the addition, the reaction mixture was refluxed for an hour at 90 °C, and then cooled. White crystals of thiocarbohydrazide (TCH) separated, recrystallized from hot water, and dried (M.P - 170 °C). In the later stage, about 23 g of TCH was added to 170 ml of boiling water in a beaker and 14 g of pyruvic acid was added to it slowly with constant stirring. Light yellow crystals of AMMOT were separated and the same is recrystallized from ethanol (M.P - 80 °C). The refluxing of AMMOT with 4-hydroxy-3-methoxybenzaldehyde in ethanolic medium yields yellow crystalline Schiff base 4-[(4-hydroxy-3-methoxybenzylidene) amino]-6-methyl-3-thioxo-3,4-dihydro-1,2,4-triazin-5(2*H*)-one (MHMMT). The product is filtered, washed with cold ethanol and recrystallized from ethanol. Yield 80%; m p: 120–122 °C. The scheme of synthesis is given as (Figure 1) [12].

2.3. Synthesis of metal complexes

The solid complexes of Fe(III), Co(II), Ni(II), Cu(II) and Zn (II) were prepared as per the following procedure. To a hot (1:1) aqueous/ethanolic solution of acetates of Co(II), Ni(II), Cu(II), Zn(II) and nitrate of Fe(III) (1mmol), hot ethanolic solution of ligand (2mmol) was added drop by drop with stirring. The resulting mixture was then refluxed for 4 h. Then the solution was cooled, the complex separated was filtered, washed with water, ethanol, acetone, and finally dried. The yield of the metal complex was in the range of 60–70 %.

2.4. In silico biological screening studies

The pre-requisite parameters of drug discovery like the drug-likeness, bioactivity scores, and ADMETox prediction of ligand and metal complexes were determined online using www.molinspiration.com and http://www.lmmd.org/database/cheminformatics websits [13]. Chemical structures and SMILES notations for the molecules were obtained using Chemdraw ultra software. These SMILES were then uploaded to the online software to calculate various molecular properties like logP, topological surface area (TPSA), number of hydrogen bond donors and acceptors, etc. and to predict bioactivity scores towards various drug targets like enzymes, nuclear receptors, kinase inhibitors, GPCR ligands, and ion channel modulators, etc. and to study various pharmacokinetic properties like ADMET (absorption, distribution, metabolism, excretion, and toxicity) of the ligand as well as complexes [14].

2.5. Prediction of Probable Activity Spectra of Substances – PASS online software

The biological and pharmacological utilities of a compound which reflects the interaction of the compound with various biological entities can be explored using PASS (Prediction of Probable Activity Spectra of Substances) analysis [15], a computer-based online software www.pharmaexpert.ru/passonline. This helps to screen the biological activities of chemical structures based on the structure-activity relationship. It compares the structure of the chemical entity with a training set consisting of more than 46,000 drugs, drug-candidates, and lead compounds. The biological activity is expressed in terms of probability values Pa (probable activity) and Pi (probable inactivity). It has been proposed that structures with Pa greater than Pi were the only compounds considered for a particular pharmacological activity [16]. If the Pa value for a

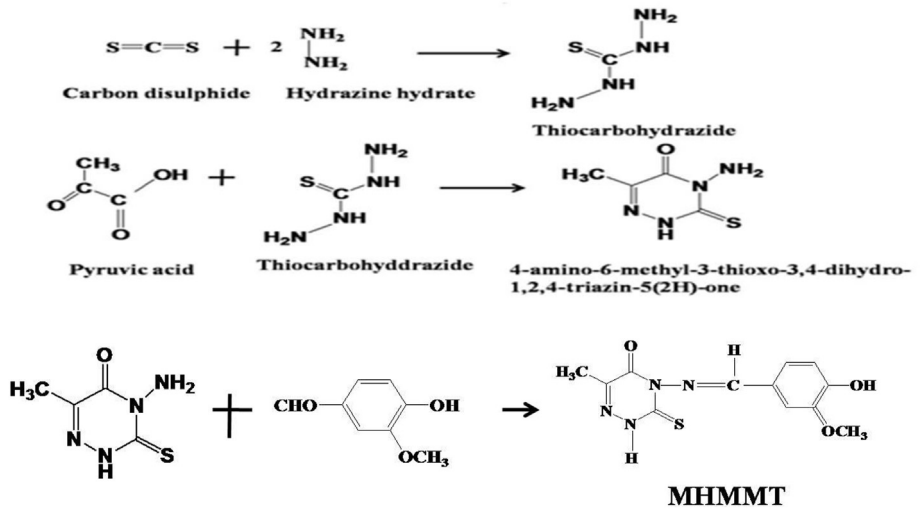

Figure 1. Synthesis of ligand MHMMT.

particular activity is greater than 0.5, the compound will probably show biological activity on *in vitro* analysis. It has been found that depending on the nature of metal ion and ligand, the probability of showing a particular activity differs.

2.6. In vitro antimicrobial studies

The compounds were evaluated for in *vitro* antibacterial and antifungal studies by the disc diffusion method and the procedure is as follows: Primarily, the bacterial and fungal stock cultures were inoculated in broth media followed by incubation at 37 °C. The standardized inoculums are then inoculated in the aseptically prepared plates and allowed to dry at room temperature. Each plate was divided into 4 parts and in each part, sample discs and standard discs were placed and refrigerated at 4 °C for the diffusion of the drug. Incubated at 37 °C for 24 h for bacterial study and 28 °C for 48 h for fungal studies and the diameter of the zone of inhibition was measured [17]. The in vitro antibacterial tests were performed on MTCC bacterial strains like *Escherichia coli (MTCC42) (gram negative), Bacillus subtilis (MTCC121)* and *Micrococcus luteus* (MTCC 7950) (gram positive) and in vitro antifungal screening tests were performed on fungal strains like *Aspergillus niger (MTCC 282),and Candida albicans (MTCC183)*

2.7. In vitro anticancer studies – MTT assay

In vitro anticancer studies of Fe(III) complexes were conducted by MTT assay. It is one of the most frequently used assays for evaluating the metabolic activity of cells which measures cell viability and proliferation. The reduction of yellow tetrazolium salt 3-(4,5-dimethylthiazolyl-2)-2,5-diphenyl tetrazolium bromide (MTT) occurs in metabolic active cells by the action of NADH and NADPH dependent dehydrogenase enzyme to produce purple coloured formazan and is solubilized in DMSO and quantitatively determined by spectrophotometric methods. MCF-7 cell lines purchased from the National Centre for Cell Science, Pune, were kept as per the standard conditions [18]. The cell lines in the log phase were seeded into 96-well plates having a concentration of 1 × 104 cells/well, which were incubated overnight at 37 °C. The cells were then treated with different concentrations of drug candidates. The control was also cultivated in the same condition without complex. The cells were incubated for 48 h and MTT assay was carried out. A stock solution of 5 mg/mL of MTT was prepared; 100 μL was added to each drug candidate treated wells and incubated for 4 h. The purple-coloured formazan crystals obtained were dissolved in 100 μL of DMSO and spectrophotometrically determined at 620 nm in a multi-well ELISA plate reader (Thermo, Multiskan).

2.8. In vitro antidiabetic studies – α-amylase inhibition studies

α-amylase inhibition studies were carried out by conventional starch-iodine method which works on the principle of hydrolysis of starch by α-amylase [19]. The starch solution without α-amylase shows a highly intense blue colour (blank) B. But the solution with α-amylase, without any metal complexes, will be almost colourless (control) C and the introduction of metal complexes will retain some blue colour for starch with iodine indicating the inhibition of α-amylase activity (A). 20 μl of α-amylase solution (1 mg/mL) was mixed with 390 μL of phosphate buffer (0.02M phosphate buffer pH 7.0 containing 0.006 M NaCl, pH 7.0) containing different concentration of solutions of complexes in DMSO. After incubation at 37 °C for 10 min, 100 μL of 1 % starch solution was added, and the mixture was again incubated for 1h. This is followed by the addition of 0.1 mL of 1% iodine solution and 5 mL distilled water, the absorbance of the resulting solution was taken at 565 nm. Sample, substrate, and α-amylase blank determinations were carried out under the same reaction conditions. Inhibition of enzyme activity was calculated as (%) = (A-C) X100/(B–C), where, A = absorbance of the sample, B = absorbance of blank (without α-amylase), and C = absorbance of control (without starch).

2.9. Molecular docking studies

In silico docking studies were performed using Autodock 4.2 version and the images are rendered using Accelry's Discovery Studio Visualizer v 4.0 interface [20]. The crystal structure of the target enzyme/protein was obtained from the RCSB protein data bank. The missing atoms in the crystal structure were repaired using the repair command module of Autodock. Before docking, the enzyme/protein structure was modified by deleting the water molecules and by adding hydrogen atoms for exact ionization and tautomeric states of amino acid residues and was used for semi-flexible docking. The ligand molecules were drawn using ACD chemsketch software. The energy minimization of ligand and target entity was done in Steepest Descent and Conjugate Gradient methods using Accelrys Discovery Studio (Version 4.0, Accelrys Software Inc.) [21]. The minimization was carried out with biomolecular simulation programme CHARMM (Chemistry at Harvard Macromolecular Mechanics) force field [22]. Lamarckian genetic Algorithms (LGA) were used as docking engine and all the docking parameters were set to default [23]. After each run, Autodock reports the best docking solution with IC50 values, and the results are obtained based on cluster analysis. After 10 docking modes of LGA cluster analysis, the lowest energy docking mode with IC50 values was selected for simulation. Every compound was allowed to have active rotatable bonds to make them flexible.

3. Results and discussion

The analytical data of the prepared ligand and its Fe(III), Co(II), Ni(II), Cu(II) and Zn (II) complexes were presented in Table 1. All complexes were found to be stable, non-hygroscopic solids, insoluble in water, and ethanol but soluble in organic solvents like DMF, DMSO, etc. It can be seen that there is a close agreement between the experimental values and calculated values of the element percentage of the proposed structures. Except Co(II), all other metal complexes form in the mole ratio 1:2 (M:L) whereas Co forms a 1:1 complex.

3.1. ^{1}H (proton) NMR spectra of MHMMT and Zn complex

The ^{1}H (proton) NMR spectral comparison of MHMMT and the diamagnetic Zn(II) complex using TMS as an internal standard furnishes useful information about the proton environment of ligand and also its mode of ligation in the complex and the same are given in (Figure 2). The spectra of ligand show a sharp singlet peak at δ 8.4 ppm which has been attributed to the presence of azomethine proton (CH = N) and a multiplet within the range of δ 7.2–7.4 ppm for aromatic protons. A dominant peak at δ 13.6 ppm suggests the existence of the thiol (SH) form of the ligand in the solution phase [24, 25]. The singlet observed at δ 2.1 ppm is due to the resonance of the methyl group, and at δ 3.8 ppm due to that of the methoxy group. The hydroxyl group has appeared as a singlet at δ 6.8 ppm. A comparison of 1H NMR spectrum of Zn(II) complex of MHMMT has shown a slight upfield shift in azomethine signal and appears at δ = 8.289 ppm pointing out the involvement of N in coordination [25, 26]. The peaks due to SH group δ = 13.6 ppm in the ligand indicating thiol-thione tautomerism is found to be absent in the spectra of Zn complex indicating the coordination of ligand through S atom of SH group via deprotonation [24]. The peaks due to methoxy protons, phenolic OH group, and aromatic hydrogen remain almost unchanged in the complex indicating the non-involvement of these groups in coordination.

3.2. IR spectra

The binding sites of ligand to metal ions can be best found out by the comparison of IR spectra of ligand and complexes. The IR spectra of

Table 1. Analytical data of transition metal complexes of MHMMT.

compounds	Analysis percentage exptl. (theoretical)				
	C	H	N	S	M
$Fe(L-H)_2(NO_3)$ (H_2O) (735) (Oh) $C_{24}H_{24}O_{10}N_9S_2Fe$	39.65(39.18)	4.07(3.26)	17.93(17.14)	9.15(8.70)	7.01(7.59)
$Co(L-H)OAc.H_2O$ (427) (Td) $C_{14}H_{16}O_9N_4SCo$	35.6(39.34)	3.75(3.74)	14.35 (13.11)	8.95(7.49)	14.02(13.81)
$Ni((L-H)_2.2\ H_2O$ (676) (Oh) $C_{24}H_{26}O_8N_8S_2Ni$	41.8(42.60)	3.62(3.84)	16.34(16.56)	9.21(9.46)	8.39(8.57)
$Cu((L-H)_2$ (645) (SP) $C_{24}H_{22}O_8N_8S_2Cu$	43.78(44.65)	3.19(3.41)	17.05(17.36)	9.73(9.92)	9.52(9.71
$Zn((L-H)_2$ (647.35) Td $C_{24}H_{22}O_8N_8S_2Zn$	43.12(44.5)	4.1(3.39)	18.1(17.30)	9.95(9.89)	9.10(10.04)

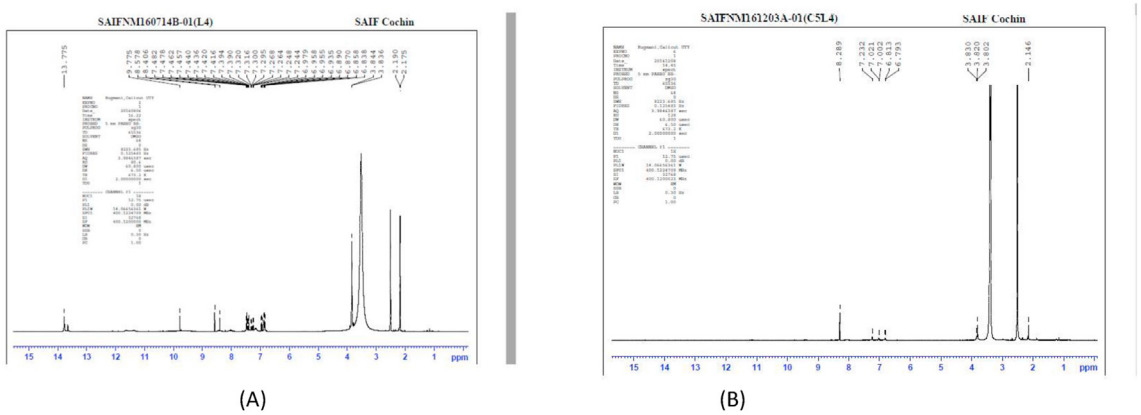

Figure 2. ^{1}HNMR spectra of (A) MHMMT (B) MHMMT-Zn Complex.

ligand, MHMMT shows three strong absorptions at 3413, 3169, and at 1598 cm^{-1} corresponds to ν(O–H), ν(N–H), and azomethine ν(HC = N) stretching vibrations respectively. The existence of another strong band around 1199 cm^{-1} can be ascribed to ν(C=S) stretching vibration indicating the possibility of thiol-thione tautomerism in the ligand. The SH stretching region around 2500 cm^{-1} of the spectrum are devoid of any peaks. So combined NMR and IR spectra suggest thiol-thione tautomerism in MHMMT, preferably thione form in the solid-state. Similar results of the existence of preferable thione form in the solid-state of thioamide groups are reported earlier also [27, 28]. The coordination sites of ligand to the metal ions can be best studied by comparing the IR spectra of ligand and complexes (Figure 3), Table 2. Complexation alters the stretching frequency of the C=N bond suggesting the coordination of ligand to metal ions through azomethine nitrogen atom [29]. The disappearance of peaks due to υ(N–H) at 3169 $cm^{-1}$and υ(C=S) at 1199 $cm^{-1}$and the appearance due to υ(C–S) around 600–700 cm^{-1}suggested the existence of thiol-thione tautomerism which is also confirmed by NMR studies. On complexation, deprotonation of thiol group takes place followed by coordination via sulphur atom. This was further supported by the appearance of new bands of υ(M-S) and υ(M-N) around 350–550 cm−1 [25] in the spectra of Fe(III), Co(II) and Ni(II) complexes of MHMMT. The peaks in the region 3300–3500 cm^{-1} and 750–850 cm^{-1} indicate the presence of coordinated water molecules [30]. Strong peaks at 1740 cm^{-1} in Co(II) complexes were assigned to the acetate group. The presence of nitrate groups was confirmed by the peaks at (1460 and 1304 cm^{-1}) in the Fe-MHMMT complex. The lower value of separation between the two peaks denotes the monodentate nature of nitrate groups [31]. The thioamide band I remain unaltered in the complexes, so a noninvolvement of N of the thioamide group is expected in complexation. The shift of about 50–100 cm^{-1} towards the lower wavenumber side for the thioamide band IV on complexation supports bonding between metal ions and S [32]. Thus, the IR spectral data suggest that the ligand MHMMT as a N, S donor bidentate ligand coordinating with the sulphur atom of thioamide group of 1,2,4-triazine ring through deprotonation, and azomethine nitrogen atom. It also indicates the monodentate coordination of the acetate group and the nitrate group.

3.3. Electronic absorption spectra

Electronic spectroscopy in combination with magnetic moment studies is an important tool in the structure elucidation of transition metal complexes. The λ_{max}, their possible assignments (Figure 4) and calculated ligand field parameters for MHMMT and its complexes depicted in Table 3 helps to predict the extent of covalent bonding and geometry of the complexes. Two intra ligand absorption bands were observed by the ligand MHMMT at 267 and 333 nm which is assigned to π-π* transitions of aromatic rings and n- π* transition of azomethine and carbonyl groups [33]. In the absorption spectra of complexes, the band at 333 nm due to n- π* transition shows a significant shift and change in intensity which confirms the ligand MHMMT with metal ions via azomethine nitrogen. Fe(III), a d5 system with lowest energy term 6S splits in an octahedral field to 6A1g ground state. The higher levels 4G, 4P, etc. are of multiplicity 4, so all transitions of Fe(III) systems are double forbidden (spin, as well as Laporte, forbidden), so the electronic spectral bands will be extremely weak. In the Fe complex, three absorption maxima are obtained and they can be assigned to various transitions as

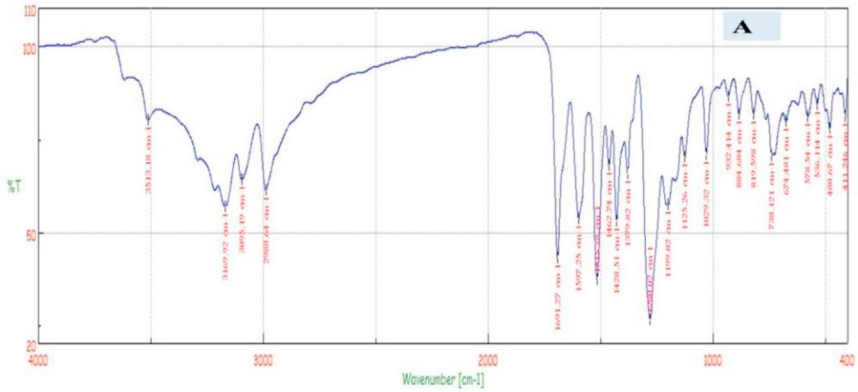

(A)

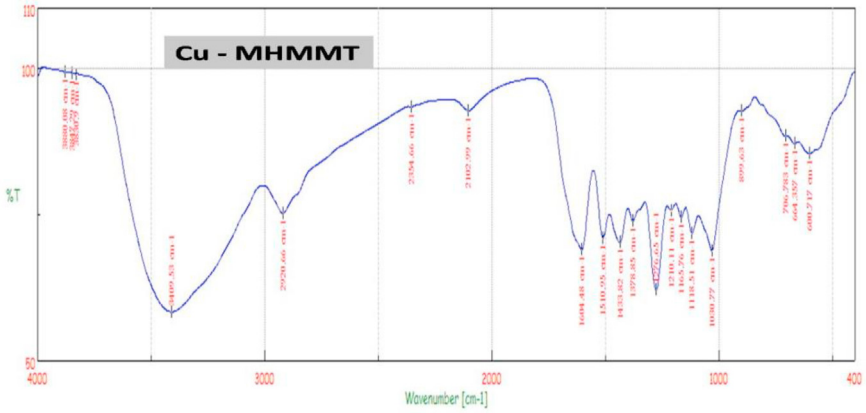

(B)

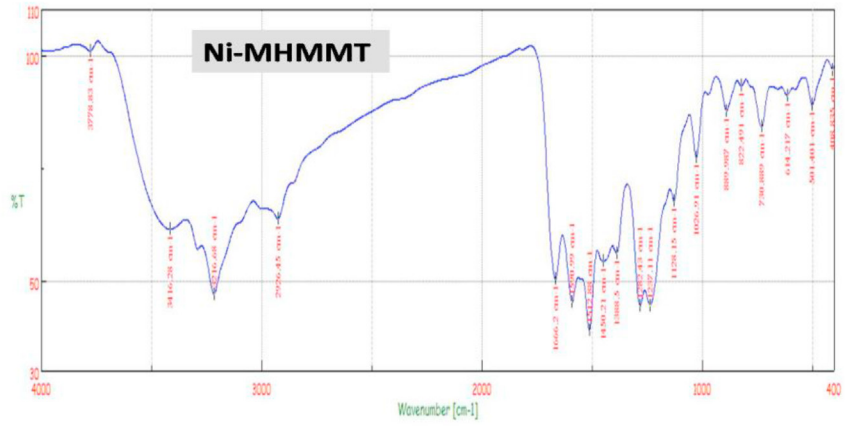

(C)

Figure 3. IR spectra of (A) MHMMT (B) Cu-MHMMT complex (C) Ni-MHMMT complex.

given in Table 3. The spectrum of Co-MHMMT complex exhibited d-d transitions at 459 and 606 nm and are attributed to4A2→4T1(P) and 4A2→4T1(F) transitions and are characteristic of tetrahedral geometry of complexes. By using band fitting equations of Lever et al. [34], the ligand field parameters can be calculated using the equations υ1 = 10 Dq, υ2 = 18 Dq and υ3 = 12 Dq + 15 B. The Racah parameter (B) values of 719 cm−1 which is less than B0value for free Co(II) ion (971 cm−1) suggests overlapping of orbitals as well as electron delocalization in the metal ion. β value of 0.74 pointed out a covalency of 26 % in the complex. The Ni(II) complex shows the electronic absorption peaks with the corresponding transitions as given in Table 3 suggested octahedral geometry for Ni(II) complex. The band fitting calculations provide B value 898 cm−1 less than that of free Ni(II) ion (1030cm−1). As presented in Table 3 Cu-MHMMT gave three bands at 362 nm, 433 nm, and a broadband at 606 nm. The first two bands can be due to charge transfer and the broadband at 606 nm can be ascribed to a combination of 2B1g→2Eg and

Table 2. Important infrared spectral bands (cm^{-1}) and their tentative assignments for MHMMT and its complexes.

compound	υ (O–H)/N–H υ(H_2O)	υ (C=N)	thioamide I & II	υ (C–O)	thioamide III & IV	δ (phenolic O–H)	υ (C–S)	υ (M-N)	υ (M-S)	Coordinated water/ Nitrate/OAc
MHMMT	3413, 3169	1598	1515 1428	1280	1125 884	1380	–	–	–	–
$Fe(L-H)_2.NO_3.H_2O$	3432, 3377	1591	1512 1460	1281	1120 862	1384	616	463	418	782, 1460, 1304
Co(L–H) OAc. H_2O	3431, 3396	1590	1509 1458	1285	1121 864	1376	628	464	428	734, 1730
$Ni((L-H)_2 2H_2O$	3414, 3216	1591	1513 1450	1282	1128 822	1389	614	501	408	730
$Cu((L-H)_2$	3409	1604	1510 1433	1276	1118 706	1378	604	482	453	–
$Zn((L-H)_2$	3425	1590	1512 1450	1282	1128 790	1388	614	501	408	–

2B1g→2A1g transitions [35] suggesting a square planar structure for Cu(II)-MHMMT complex [36].

3.4. Magnetic susceptibility studies

Magnetic susceptibility studies were determined as per the procedure explained in the experimental section and the results obtained are given in Table 3. The effective magnetic moment, (μeff) values were calculated from susceptibility using the relation

$$\mu_{eff} = 2.828\sqrt{\chi_M^{corr}T}\ BM \quad (1)$$

where χ_M^{corr} is the molar susceptibility corrected for diamagnetic correction using Pascal's constants [37], T the absolute temperature in K. The Fe(III) complex possesses a magnetic moment of 4.82 BM which is lower than that of high spin octahedral and is much higher than that of the low spin octahedral complex. It has been suggested that in an octahedral field for a d^5 system with $^6A_{1g}$ configuration like Fe^{3+}, a spin state equilibrium as well as the anti-ferromagnetic exchange is possible, which results in subnormal magnetic moment values [38, 39]. This tentative explanation tends us to expect an octahedral environment around Fe(III) ion. The Co(II) complex has a magnetic moment value of 4.65 BM higher than that expected for a tetrahedral Co(II) complex without any orbital contribution. The exceptionally high value can be due to the mixing between the ground and excited states due to spin-orbit coupling and thus gets some orbital contribution [40]. The Ni(II) complex has a magnetic moment value of 3.2 BM, which is consistent with the reported values for octahedral Ni(II) complexes [41].

The Cu(II) complex with a magnetic moment of 1.83 BM which is slightly higher than the spin only value of 1.73 BM and this may be due to spin-orbit coupling followed by lowering of symmetry [42] and is reliable with square planar geometry around Cu(II) ion.

3.5. Thermal analysis

Thermal analysis of the metal complexes of MHMMT was performed out within a temperature range of 40–800 in an inert atmosphere. In most cases, the decomposition found to occur in two or three stages. It is

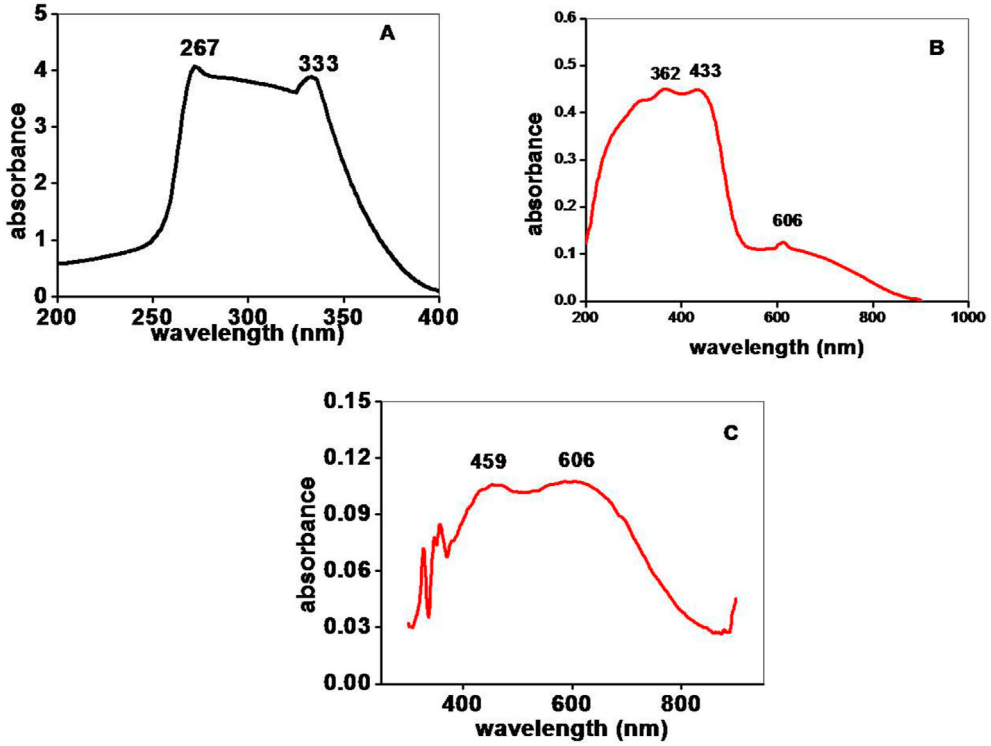

Figure 4. Electronic spectra of (A) MHMMT (B) Cu(II) complex (C) Co(II) complex.

Table 3. Electronic spectral bands with probable assignments.

compound	Band position nm	Assignment	Dq cm^{-1}	B	$\beta = B/B_0$	Magnetic moment μ_{eff} BM
MHMMT	267 333	$\pi - \pi^*$ $n - \pi^*$	–	–	–	
Fe-MHMMT	344 510 277	$T_{2g} - \pi^*$ $^6A_{1g} \rightarrow {}^4T_{1g}$ $^6A_{1g} \rightarrow {}^4T_{2g}$	898.7	817	0.81	4.82
Co-MHMMT	1091(ca) 606 459	$^4A_2 \rightarrow {}^4T_2$ $^4A_2 \rightarrow {}^4T_1(F)$ $^4A_2 \rightarrow {}^4T_1(P)$	916.7	719	0.74	4.65
Ni-MHMMT	820(ca) 454 356	$^3A_{2g} \rightarrow {}^3T_{2g}(F)$ $^3A_{2g}(F) \rightarrow {}^3T_{1g}(F)$ $^3A_{2g}(F) \rightarrow {}^3T_{1g}(P)$	1218	898	0.87	3.20
Cu-MHMMT	362 433 606 (b)	CT CT $^2B_{1g} \rightarrow {}^2E_g$				1.73
						–

visible from the thermograms that up to 200 °C, the various phenomenon's can be assigned like the elimination of some gases adsorbed or some volatile substances produced by the evaporation during complex synthesis, removal of adsorbed and coordinated water molecules, etc. The final stage in the decomposition of complexes is oxide formation [43]. The thermograms of Fe(III), Co(II) and Ni(II) complexes of MHMMT shows the presence of coordinated water molecules. In the thermogram of Fe(III) complex, the mass loss in the region 80–150 °C corresponds to the loss of water molecules with an observed mass loss of 3 % is in good agreement with the calculated value of 2.5 %. The mass loss of 43.2% (theoretical 40.6%) in the temperature range 440–570 °C corresponds to the loss of ligand moiety. After 600 °C, only metal oxide remains with a residue percentage of 10.9 (calculated value: 9.9 %).

The thermogram of cobalt complexes of MHMMT decomposes in three stages. In the first stage around 50–140 °C with a loss of 5.51 % agrees well with the theoretical water loss percentage of 4.21. This anhydrous complex decomposed into metal oxide via two intervening stages where the loss of organic part in the temperature range 250–400 °C and 400–700 °C leaving behind CoO as the residue. The thermogram of Ni-MHMMT shows the mass loss (found 4.7 (theoretical 5.3 %)) attributing to the loss of two water molecules in the temperature range 50–170 °C. In the second stage of decomposition of 250–500 °C, loss of organic matter occurs, and finally, the residue percentage is that of NiO (calculated 11%, found 14.2 %). The copper complex of MHMMT is stable up to 200 °C implying the absence of coordinated water molecules in the complex. The complex decomposed in two stages which involve the partial loss of organic matter and finally the complete loss of ligand to give CuO as residue.

3.6. Electron spin resonance spectra

The X-band of solid-state ESR spectra of Cu(II) –MHMMT complex was carried out in DMSO solvent at liquid nitrogen temperature (77 K) and are given in (Figure 5). The analysis of spectrum gives g values for Cu-MHMMT complex as $g\| = 2.24$, $g\perp = 2.05$ ie., $g\| > g\perp > 2.0023$ suggest the covalent character of M-L bond with the unpaired electron of Cu localized in dx^2— dy^2orbital of Cu(II) ion characteristic of square planar stereochemistry [44]. The geometric parameter G, which measures the exchange interaction between the Cu(II) centres in polycrystalline compounds, is determined using the equation

$$G = \frac{g_{//} - 2.002}{g_{\perp} - 2.002}$$

As per Hathaway [45], if the value of G is greater than four, the exchange interaction between Cu(II) centres is can be neglected, whereas if the value of G is less than 4, there is a considerable exchange interaction. In the present case, the calculated $G = 4.95 > 4$, suggests a parallel alignment of the local axis or a slight misalignment. The magnetic interaction between Cu(II) ions in its complex in the solid-state are negligible [46].

3.7. Structure of metal complexes

A detailed study of results of the physical and spectral characterization techniques described above, a tetrahedral geometry was suggested for Co(II) and Zn(II) complexes, an octahedral structure for complexes of Ni(II) and Fe(III) and a square planar one for Cu(II) complex and the suggested structures of complexes are given as (Figure 6).

3.7.1. Virtual screening of pharmacological behaviour

The virtual screening of some pharmacological behaviour like drug-likeness, bioactivity score, ADMEtox studies, PASS spectrum, etc. of the ligand as well as metal complexes was done in an *in-silico* manner using various online tools like www.molinspiration.com, http://www.lmmd.org/database/cheminformatics, www.pharmaexpert.ru/passonline as described elsewhere.

3.7.2. Bioactivity score prediction and verification of Lipinski's rule of 5

The beneficial interaction of drugs with various biological targets like enzymes, ion channels, receptors, etc. in living beings describe the pharmacological activities of drugs. The bioactivity scores like binding to G-protein coupled receptor ligand (GPCRL), nuclear receptor ligand (NRL), ion channel modulation (ICM), kinase inhibition (KI), protease inhibition (PI), enzyme inhibition (EI), etc. and bioavailability of ligand, as well as complexes, were predicted by subjecting them to calculations using a web-based tool, *Molinspiration* and the results are displayed in

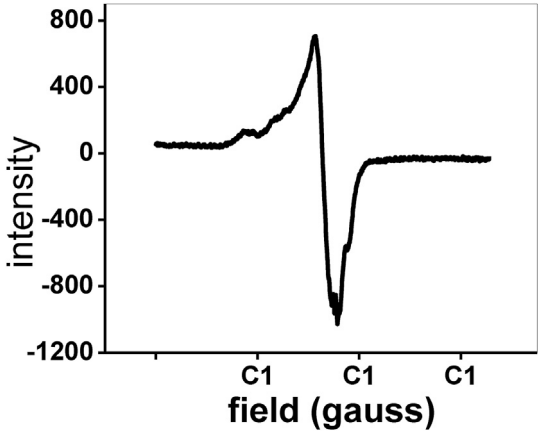

Figure 5. ESR spectra of Cu(II) complex.

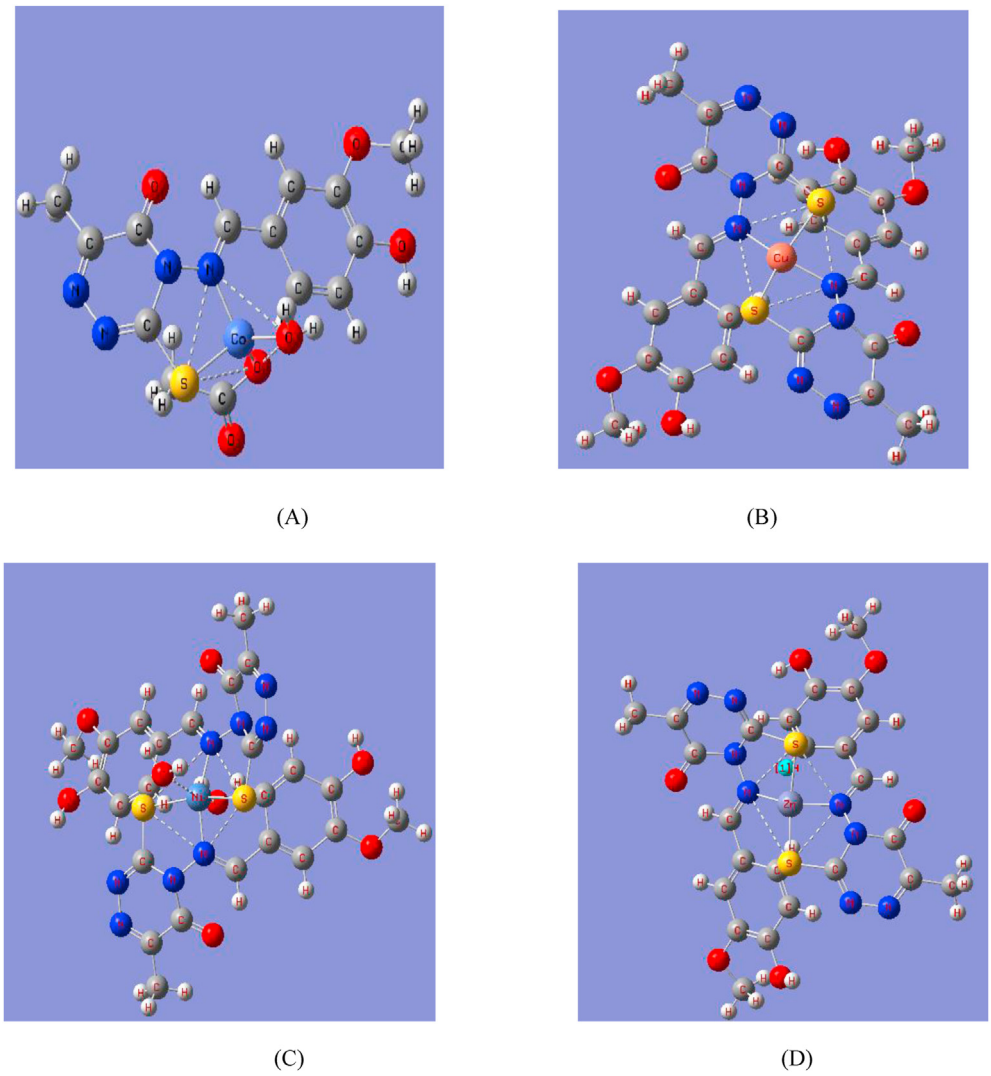

Figure 6. Proposed structure of metal complexes: (A) Co(II), (B) Cu(II), (C) Ni(II), (D) Zn(II).

Table 4. It has been suggested that metal complexes with bioactivity scores greater than zero are highly bioactive in nature whereas those with scores between −5.0 to 0 have moderate activity and if the score is less than −5.0, then they are inactive [47]. It can be observed from Table 4 that ligand as well as metal complexes have values within −1.42 to −0.01, so they are expected to have moderate activity [48]. They are expected to retain such properties as demanded for them to behave as potential drugs with some alterations in their chemical structure [49].

Lipinski's rule of five (RO5), a benchmark in drug design and development, helps in the description of molecular properties of drug candidates which gave insight into various pharmacokinetic parameters like absorption, distribution, metabolism, and excretion (ADME) for predicting the success of an orally introduced drug's journey through the body towards the site of action. The rule predicts the oral activity of a drug candidate in connection with a certain molecular parameter like logP (partition coefficient), molecular weight, number of hydrogen bond acceptors and hydrogen bond donors, and polar surface area. According to RO5, an orally active drug candidate should have log P $\leq$ 5, number of hydrogen bond acceptors $\leq$10, number of hydrogen bond donors $\leq$5, and molecular weight $\leq$500 [50]. Generally, an orally active drug should not show any violation of these rules. In the present analysis, the values of milLogP, TPSA, molecular weight, and other parameters for ligand as well as complexes are calculated and the same are also presented in Table 4. It can be seen that ligand and complexes are having milLogP

Table 4. Validation of Lipinski's rule and bio activity scores as obtained from Molinspiration software.

compound	Druglikeness			Bioactivity scores					
	milogP	TPSA	Nviolations	GPCRL	ICM	KI	NRL	PI	EI
MHMMT	0.19	93	0	−1.33	−1.17	−1.16	−1.28	−1.47	−0.91
Fe-MHMMT	-6.00	239	2	−0.39	−1.05	−0.73	−0.80	−0.38	−0.47
Co-MHMMT	−5.41	130	0	−0.29	−0.29	−0.36	−0.30	−0.34	−0.06
Ni-MHMMT	−5.97	190	3	−0.29	−0.70	−0.46	−0.49	−0.31	−0.28
Cu-MHMMT	−5.53	158	2	−0.20	−0.51	−0.36	−0.42	−0.20	−0.22
Zn-MHMMT	−5.36	158	2	−0.20	−0.51	−0.36	−0.42	−0.20	−0.15

values in the range −6.00 to 0.19 (≤5), which is within the tolerable limit of a drug candidate to infiltrate through biomembranes and are displaying good bioavailability as per Lipinski's Rule [51]. The ligand and its Co(II) complex show any violation of Lipinski's rule whereas other complexes show violations. So the ligand and Co(II) complex can be considered as oral therapeutic molecules as per RO5. But the recent developments in drug discovery have increased the chemical space for oral druggable candidates beyond Lipinski's Rule of 5 (bRo5) by considering target interaction and to incorporate various natural products rich in activities [52]. So Ni(II), Cu(II), Zn(II), and Fe(III) complexes also can be included in the chemical space of bRo5 with some modifications.

3.7.3. ADMETox prediction

ADMETox prediction involves the study of the absorption, distribution, metabolism, excretion, and toxicity of drug molecules starting from the site of administration, absorption into the system wide circulation, motion in the blood and excretion and it is a major component of pharmacokinetic studies. The online software ADMETSAR methodology [53] utilizes various absorption and excretion models like Caco-2 cell permeability, Blood-Brain Barrier (BBB) penetration, Human Intestinal Absorption (HIA), and toxicity parameters like carcinogenetic, LD_{50} dosage, etc. The predicted ADMET data for the ligand as well as metal complexes are summarized in Table 5 The ADMET properties revealed that metal complexes are having high absorption, distribution properties indicated by high HIA, BBB, $Caco_2$ permeability values in comparison with ligand and it implies the more favourable pharmacokinetic properties for metal complexes compared to the ligand. Carcinogenic profile of ligand as well as metal complexes also displayed a non-carcinogenic nature. The important information gathered from ADMETSAR is the computed median lethal dose (LD_{50}) dosage in the rat model which helps in deciding the lethalness of a compound. Compounds with a lower dose of LD_{50} are more lethal compared to those with higher LD_{50} values. The LD_{50} values of studied complexes are more than that of commonly used drug streptomycin (LD_{50} = 1.8409 mol/kg).

3.7.4. Biological activity: In silico PASS analysis

As a preliminary to *in vitro* biological screening studies, the ligand as well as complexes were screened *in silico* with the help of a robust analysis based on structure-activity relationship. The most probable biological activities as obtained from a computer-based PASS online programme of MHMMT and its complexes are tabulated in Table 6. Synthesized ligand as well as complexes were found to have a wide spectrum of pharmacological activities like insulysin inhibition, antineoplastic activity, Mcl-1 antagonist, Cytidine deaminase inhibition, Maillard reaction inhibition, CYP2H substrate, Antischistosomal, etc. The ligand and its metal complexes except Fe(III) complex show insulysin inhibitor activity (anti-diabetic activity) with Pa value greater than 0.5 which suggested an *in vitro* antidiabetic activity for these compounds. The Fe(III) complex of MHMMT has a comparatively high Pa value for antineoplastic activity against breast cancer and melanoma cancer which indicated an anticancer activity for this compound. The divalent Cu and Zn complexes of MHMMT possess Pa values greater than 0.5 for antituberculosis activity which is consistent for showing in vitro antituberculosis activity.

3.7.5. In vitro biological studies

The *in silico* analysis is followed by in vitro and in vivo analysis to authenticate the results. In vitro analysis is dealt with studies of biological properties done in a controlled environment, outside of a biological organism. These studies are conducted using components of an organism isolated from their original biological environment and the studies cannot be relied upon for the whole organism analysis in a biological environment [54, 55]. So, various in vitro biological studies were also carried out.

3.7.5.1. Antimicrobial activity. The ligand along with its complexes was evaluated for their potential antibacterial inhibition efficiency against gram negative bacterial strain *Escherichia coli (MTCC42) and gram positive bacterial strains like Bacillus subtilis (MTCC121)* and *Micrococcus luteus* (MTCC 7950) by disc diffusion method as described in the experimental section. The antibacterial activity index of selected compounds is presented in (Figure 7). It is obvious from the figure that, ligand MHMMT shows moderate inhibition efficacy against both Gram-negative (*Escherichia coli, 56%)* and Gram-positive (*Bacillus subtilis* 50% and *Micrococcus luteus 31%*) bacterial species. All the studied metal complexes found to possess moderate antibacterial activity against both gram-negative and gram-positive bacterial species employed in this work. It has been found that, synthesized ligand exhibits higher antibacterial performance than complexes.

Antifungal screening were performed for the selected fungal species like *Aspergillus niger (MTCC 282),and Candida albicans (MTCC183)*. The antifungal activity assay of the compounds is presented as (Figure 8). It

Table 5. ADMETOX properties of MHMMT and its complexes studied using ADMETSAR software.

compounds	BBB	HIA	Caco-2 Permeability	Renal Organic cation transporter	carcinogenicity	LD_{50} mol/kg
MHMMT	0.5250	0.7201	0.5201	Non-inhibitor	Non-carcinogen	2.2793
Co-MHMMT	0.8444	0.9666	0..5937	Non-inhibitor	Non-carcinogen	2.6370
Ni-MHMMT	0.8333	0.9394	0.5702	Non-inhibitor	Non-carcinogen	2.6627
Cu-MHMMT	0.8117	0.8511	0.5679	Non-inhibitor	Non-carcinogen	2.6016
Fe-MHMMT	0.7552	0.9345	0.5781	Non-inhibitor	Non-carcinogen	2.5513

Table 6. Probable Activity Spectrum of MHMMT and its complexes as obtained from online software PASS online.

Activities	P_a values					
	MHMMT	Fe-MHMMT	Co-MHMMT	Ni-MHMMT	Cu-MHMMT	Zn-MHMMT
Insulysin inhibitor	0.794	0.383	0.703	0.618	0.748	0.726
Mcl-1 antagonist	0.717	–	0.510	0.243	0.618	0.584
Cytidine deaminase inhibitor	0.644			0.183	0.350	0.315
CYP2H substrate		0.712				
Antischistosomal			0.712			
Maillard reaction inhibitor	0.597		0.611	0.384	0.632	0.620
Anti tuberculosis	0.470	–	0.449	0.497	0.597	0.735
Anti neoplastic		0.799		0.330		

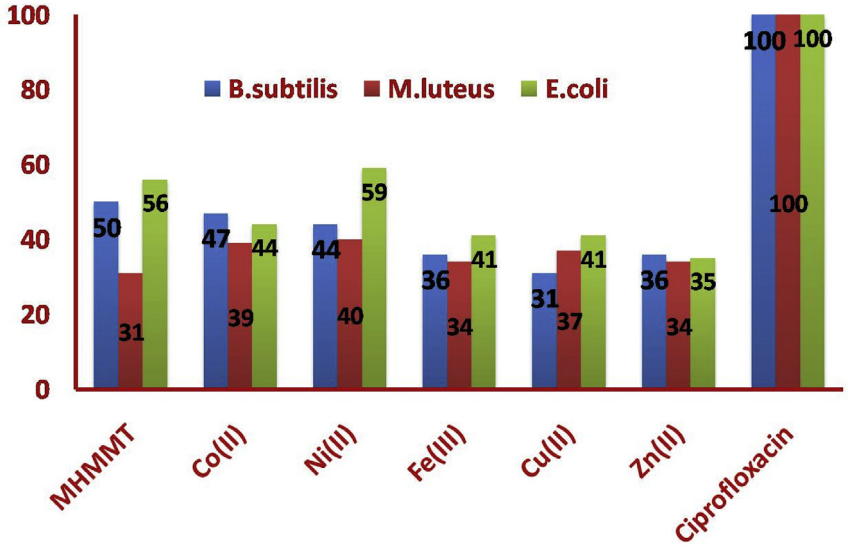

Figure 7. Antibacterial index of ligand and its complexes.

can be noticed from the figure that the ligand MHMMT and its Zn(II) complex shows excellent inhibition activities against *Aspergillus niger* (83 and 78% respectively) and *Candida albicans* (96 and 84% respectively). Considering the other metal complexes, all of them show moderate inhibition efficacies against the studied fungal species with Cu-MHMMT complex showing excellent activity with an antifungal activity index of 80% against *Candida albicans*.

So, the ligand MHMMT displays good antimicrobial efficiency in juxtaposition to its metal complexes. This can be presumably due to azomethine, hydroxyl and thiol radicals which are capable of developing hydrogen bonding interactions with cellular compartment [51]. The lesser activity of complexes may be due to their inability to penetrate through the cell wall of the microbial species thus obstructing their biological action or because of some unknown cellular mechanism by microbial enzymes after diffusion [56].

3.7.5.2. Anticancer activity. The PASS analysis has shown a comparatively higher Pa value (0.799) for antineoplastic (breast cancer) activity for the Fe-MHMMT complex. So *in vitro* cytotoxic activity and anticancer studies were carried out for Fe-MHMMT complex against human breast cancer cell line (MCF-7) using the colorimetric method of MTT assay as per the procedure given in the experimental section. The dose-dependent cytotoxic effect was observed for Fe (III) complex treated MCF-7 cell lines and is shown in (Figure 9). The concentration of complex which produces 50 % cell death and 25 % cell death gives the IC_{50} and IC_{25} values of Fe-MHMMT complex against MCF-7 cells and this value was found to be 24 μM and 13 μM respectively and is potent against MCF-7 cell lines. The changes in the morphology of MCF-7 cell lines in presence of Fe complex were analyzed using a Nikon (Japan) bright-field inverted light microscope at 40x magnification. The presence of strong blue fluorescence in the DAPI images and the cellular uptakes shown in the images (Figure 10) and (Figure 11) revealed the anticancer activity of Fe-MHMMT complex against human breast cancer cell lines MCF-7 cell lines.

3.7.5.3. Antidiabetic activity. As evident from Table 6, the Pass analysis has shown comparatively high probability (high Pa values) for insulysin inhibitor activity for MHMMT and some of its metal complexes. Insulysin, otherwise known as an insulin-degrading enzyme (IDE), is a ubiquitous zinc peptidase that is responsible for insulin catabolism, decreases insulin levels in the pancreas and results in irregularities in the blood glucose levels. So insulysin inhibition activity reduces the degradation and clearance of insulin [57]. Various studies demonstrated the feasibility of inhibiting insulysin activity as a new therapeutic strategy to treat type-2 diabetes, a complex chronic pathological condition considered as a major health problem causing morbidity and mortality for the future

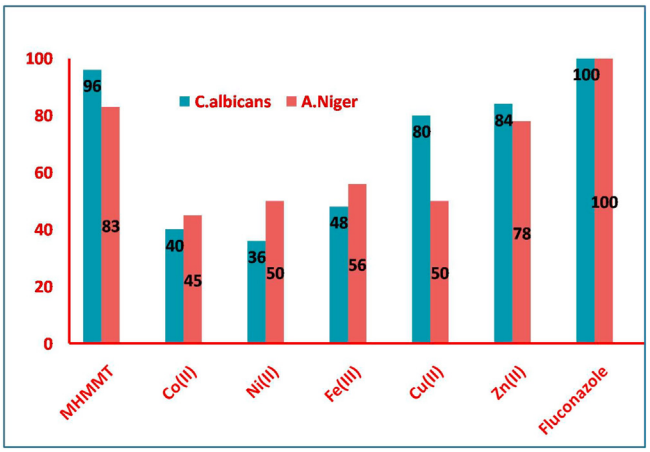

Figure 8. Antifungal index of ligand and its complexes.

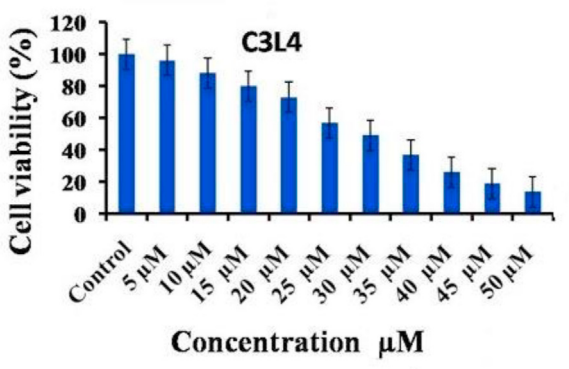

Figure 9. Dose dependent cyto toxic activity of Fe-MHMT complex against MCF-7 cell lines.

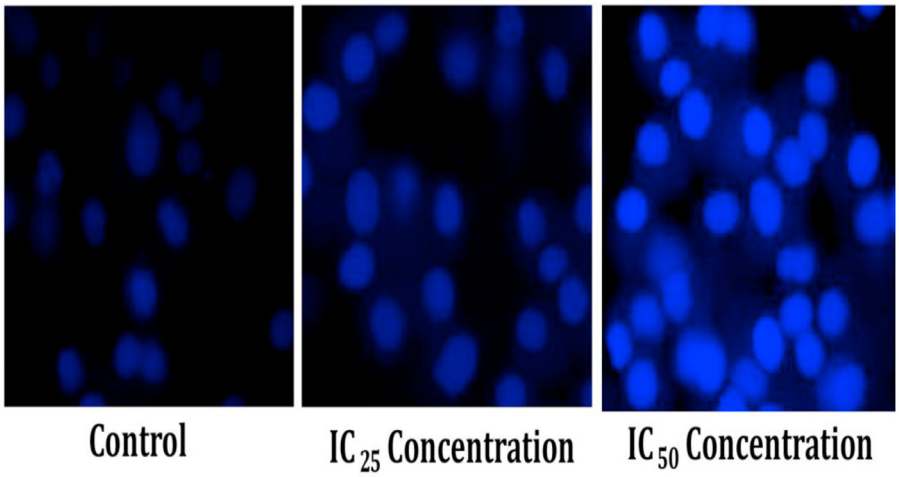

Figure 10. Bright field inverted light microscopy images (DAPI) of control cells, IC25 and IC50 of Fe-MHMMT treated MCF-7 cells.

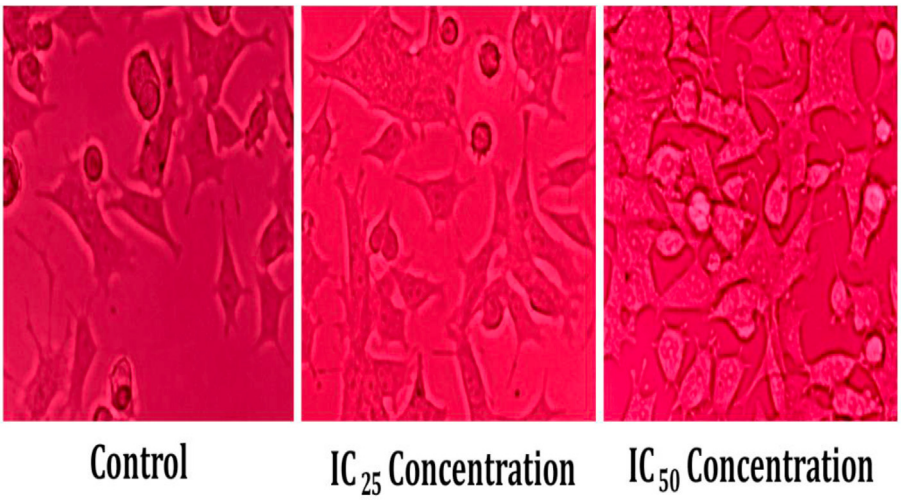

Figure 11. Fluorescence microscopic images of control cells, IC 25 and IC 50 of Fe-MHMMT treated MCF-7 cells.

worldwide. Insulysin inhibitors will provide impairments in insulin signaling which is beneficial to diabetes patients.

Type II diabetes also occurs because of carbohydrate and lipid metabolism disorders.

So along with insulysin inhibitors, the present oral therapeutic strategy for the treatment of diabetes includes the use of α-amylase inhibitor. α-amylase is a protein enzyme that hydrolyzes α-bonds of polysaccharides like starch to provide glucose and maltose. Microorganisms, some plants, and animals produce a large number of protein inhibitors that control the activity of α-amylase. These inhibitors work in an effective strategy by shutting down the postprandial rise of glucose level and are very important for diabetic patients for whom low insulin levels prevent the flow of extracellular glucose from the blood. So diabetic patients should have a low α-amylase level and α-amylase inhibitors are potential sources of antidiabetic drugs (antihyperglycemic agents). Many transition metal complexes were reported to possess an insulin-mimetic effect and α-amylase inhibition capacity.

In the light of the above knowledge, we conducted the antidiabetic studies of MHMMT and some of its complexes by the α-amylase inhibitory method depicted in section II.8. The results provided in Table 7 gives the percentage of inhibition activity for various concentrations of the ligand as well as complexes. MHMMT and its Ni(II) complex show less than 50% inhibition activity even for 300μg so they can be considered as mild inhibitors of α-amylase, whereas Co(II), Zn(II), and Cu(II) complexes show excellent inhibition activity at a concentration of 300μg. So, they can be considered as strong α-amylase inhibitors. The α-amylase inhibition activity of MHMMT and their complexes accompany the order MHMMT < Ni-MHMMT < Co-MHMMT < Zn-MHMMT < Cu-MHMMT. The better activity of complexes can be due to the incorporation of metals [58]. The enhanced activity was revealed by Cu(II) and Zn(II) in comparison to Co(II) and Ni(II) complexes. This can be explained as follows: From scientific and clinical studies, it has been reported that oxidative stress plays a major role in the pathogenesis and development of complications in diabetes [59]. The antioxidant behaviour of metals like Cu(II) and Zn(II) can reduce oxidative stress which in turn can act as good antidiabetic agents. In addition to this, the in vivo antidiabetic studies on copper complexes also revealed the enhancement of the tolerance of pancreatic β-cells against oxidative stress in presence of copper, which also supports the increased antidiabetic activity of copper complexes. Copper can also activate the phosphoinositide 3'kinase (PI3–K/Akt) pathway leading to GLUT 4 translocation which also supports the enhanced antidiabetic activity of copper complexes [60, 61, 62]. So, from this investigation of MHMMT and its metal complexes on the inhibition of carbohydrate hydrolyzing enzyme α-amylase, and along

Table 7. Antidiabetic studies of MHMMT, and its complexes Optical density of blank (without α-amylase) (B) = 0.620 Optical density for control (with α-amylase) (C) = 0.006.

Compound	Optical density at 565 nm for (A)			% of inhibition (A—C/B—C) x 100		
	50 μg	100 μg	300 μg	50 μg	100 μg	300μg
MHMMT (L1)	0.018	0.138	0.188	2	22	30
Co-L1	0.009	0.092	0.415	0.5	14	67
Ni-L1	0.021	0.033	0.283	3	5	45
Cu-L1	0.025	0.282	0.551	3	45	89
Zn-L1	0.036	0.308	0.531	5	49	86

Table 8. Docking results of selected compounds targeting α-amylase enzyme(PDB ID: 1SMD) and VEGFR 2 (PDB ID: 3VHE).

Drug target	compound	Binding Energy in Kcal/mol	Predicted IC_{50} value	Active sites with mode of interaction	
				Van der Waals	Hydrogen bonding
Alpha-amylase enzyme (PDB ID: 1SMD)	MHMMT	-6.84	9.76 uM	VAL98 LEU 162 HIS101 TYR62 HIS 299 TRP 58 ARG 195 SER 199 VAL 234	ASP 197 GLU233 LYS 200 ILE 235
	Co-MHMMT	-6.19	29.10 uM	ASP 356 HIS 305 TRP59 TYR 62	LYS 352 HIS 299 ASP 197
	Ni-MHMMT	-6.54	16.10 uM	LYS 352 ILE 51 HIS 101 GLY 304 VAL 234 TRP 58 GLU 233	GLN 63 TRP 59
	Cu-MHMMT	-7.06	6.63 uM	ALA 198 GLU 233 LEU 162 GLN 63 GLY 104 PRO 54 LYS 352 VAL 354 ASP 356	HIS 299 ASR 197 HIS 305
	Zn-MHMMT	-7.58	2.76 uM	LEU 162 GLY 306 HIS 305 GLY 309 ALA 310 VAL 234 GLU 233 ASP 236 ALA 198	GLY 308 GLY 238 LYS 200 ILE 235 HIS 201
	acarbose	-0.04	8.61 mM	ASP 236 PRO 241 SER 163 LEU 162 HIS 201 ALA 307	GLY 239 GLU 238 LEU 237 GLU 240 ILE 235 GLY 306 ASN 152
VEGFR-2-kinase	Fe-MHMMT	-5.80	36.02 uM	LEU 840 PHE 1047 GLY841 ALA 1050 LYS 871 ASP 1052 GLY 843 ALA 844 ARG 842	ARG 1051
	Lenvatinib	-8.05	1.27 Um	HIS 894 GLU 828 PHE 829 GLY 903 ILE 856 ASP 857 ASN 900 LEU 901 HIS 891	ILE 890 LEU 889 LYS 826 LEU 902

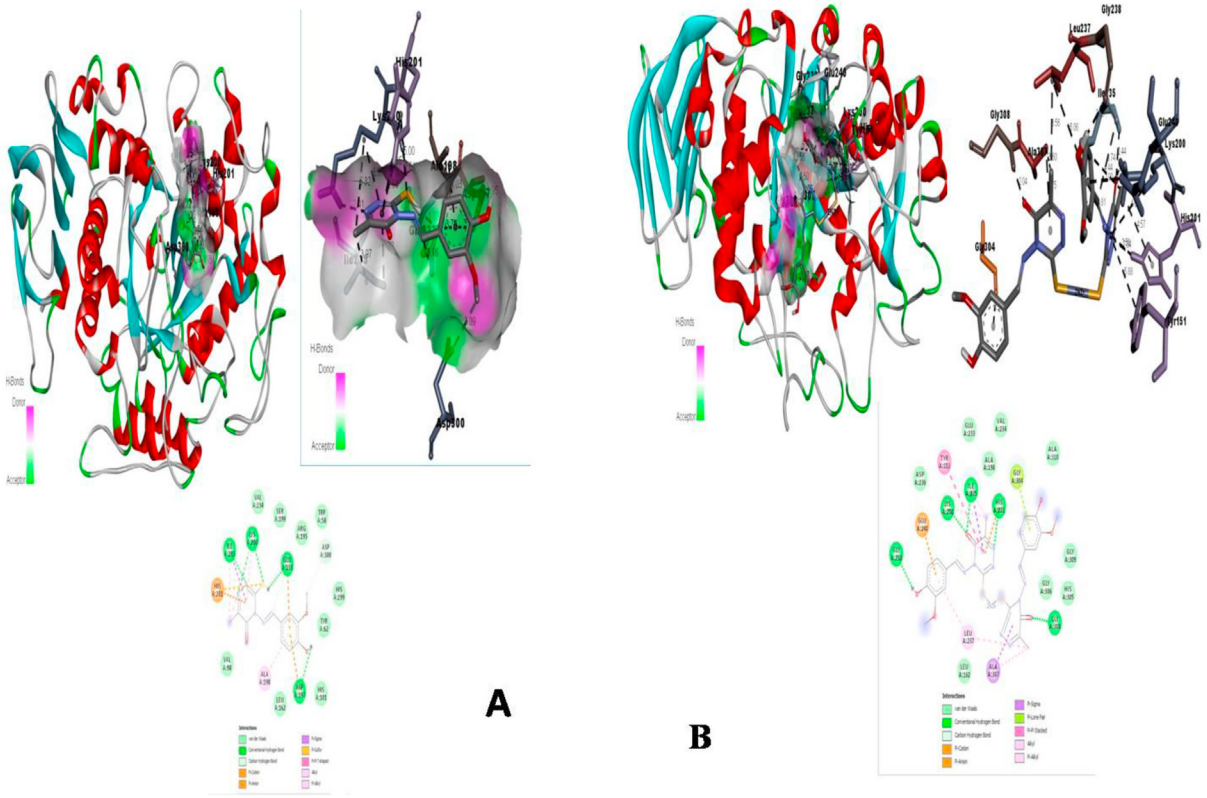

Figure 12. Snapshots of molecular docking studies of (A) MHMMT (B) Zn-MHMMT.

with the reports of preference for this in irregular bacterial fermentation of undigested carbohydrates in the intestine, it can be inferred that these complexes can act as prospective candidates for managing diabetics.

3.7.6. Molecular docking studies

Molecular docking studies were carried out using Autodock 4.2 software to model the interaction between drug molecules and proteins at atomic levels and to illustrate the fundamental biochemical process [63]. The detailed procedures of the studies are given in section II.9. Autodock helps to predict the binding site with associated binding energy and IC_{50} value of the compounds with the target domain using the protocols followed elsewhere [64, 65].

3.7.6.1. Docking studies with α-amylase enzyme and VEGFR 2-kinase as active sites. There are various routes for cancer development mainly through different enzymes, and, cyclin dependent kinase-2 (CDK-2), human topoisomerase IIa and vascular endothelial growth factor receptor-2 (VEGFR-2) are found to be the three most common ones. The vascular endothelial growth factor receptor type 2 (VEGFR-2), a tyrosine kinase linked receptor; plays an important role in normal physiological processes such as cell proliferation, differentiation, migration, and angiogenesis, which makes VEGFR-2 an attractive target for cancer. Angiogenesis is the process of formation of new blood vessels from existing vascular network which plays an important role in organogenesis, embryonic differentiation, wound repairment and reproductive functions. It is also the reason for various disorders which include tumour formation, cancers, rheumatoid arthritis etc and Vascular Endothelial Growth Factor (VEGF) take a critical part in angiogenesis process. The involvement of VEGF proteins are found to be dramatically increased in various types of human cancers and VEGF interposes its effects by binding to distinct receptors, inhibitions of actions of these receptors is supposed to be a therapeutic target in cancer treatment. By considering this, Fe-MHMMT complex was docked with VEGFR-2-kinase enzyme and MHMMT and its Co(II), Ni(II), Cu(II), and Zn(II) complexes were docked with the α-amylase enzyme (1SMD) (human salivary amylase) to validate the experimental studies and to locate the possible sites and mode of interaction. The commercially available drug molecules which are used as α-amylase inhibitors (acarbose) and VEGFR-2-kinase inhibitors (Lenvatinib) were also subjected to docking studies for comparison.

The docking parameters and corresponding binding pockets give the docking poses which help to evaluate the inhibitory activities of the studied compounds on the enzymatic action. The results of these docking studies including various docking parameters, detailed interactions between the target enzyme and compounds along with computed IC_{50} values are summed up as Table 8. The data in the table revealed the role of various kinds of interactions in the stability of ligand-receptor complexes and the important among them include hydrogen bonding, Van der Waal's and other types of interactions like π-cation, π-anion, π-alkyl, π-π stacked, etc. with various amino acid moieties in the enzyme. The respective binding energies of MHMMT, Co(II), Ni(II), Cu(II), and Zn(II), acarbose- α-amylase enzyme were found to be −6.84, −6.19, −6.54, −7.06, −7.58, and −0.04 kCal/mol respectively. In this analysis, Cu(II) and Zn(II) complexes show relatively high negative binding energies indicating their greater affinity towards α-amylase. The studied ligand MHMMT and all its metal complexes have higher negative binding energies than the standard acarbose, suggesting a higher affinity towards the enzyme in comparison with the standard. From the IC_{50} values computed from docking studies, it can be understood that the ligand as well as metal complexes are potent α-amylase inhibitors with IC_{50} in the range 2.76–29.1 μM whereas standard acarbose has an IC_{50} of 8.61 mM. This also suggests higher inhibition potential of ligand and complexes than the standard.

Considering the docking studies with VEGFR-2 kinase, the binding energy of Fe(III)-MHMMT – VEGFR-2 kinase was found to be −5.80 kCal/mol with an IC_{50} of 36.02 μM. This docking scores of the Fe-MHMMT complex indicate the potent anti-cancer activity of the compound which is found to be valid with the experimental results obtained from MTT assay.

The docking snapshots of studied compounds at the active binding site of the enzyme are represented in Figure 12. It is evident from the figures that the studied complexes have excellent binding sites to interact with the enzyme, and there are various kinds of interactions between the ligand and receptor which stabilizes the ligand-receptor complexes and inhibits the action of enzymes. The major interactions include hydrogen bonding, Van der Waal's and other types of interactions like π-cation, π-anion, π-alkyl, π-π stacked, etc. with available amino acid residues in the enzyme. Further in vivo and cytotoxic studies are required for developing them as potential drugs.

4. Conclusions

This paper discusses the synthesis, characterization, in *silico*, and in *vitro* biological screening of Fe(III), Co(II), Ni(II), Cu(II), and Zn(II) mononuclear complexes with a 1,2,4-triazine based Schiff base, MHMMT. The physicochemical, magnetic, thermal, and spectroscopic analysis revealed that MHMMT behaves as a bidentate ligand in the metal complexes coordinating through N of azomethine group and S atom of thiol group after deprotonation. The metal to ligand ratio is found to be 1:2 except that in Co(II). The various analytical studies done on complexes suggested a tetrahedral geometry for complexes of Co(II) and Zn(II) and an octahedral geometry that for Ni(II) and Fe(III). A square planar structure is suggested for Cu(II) complex. In *silico* biological screening indicates that the compounds are good drug candidates possessing diverse biological activities. The ADMETox studies show more preferred pharmacokinetic ADME properties for complexes compared to ligands with all studied compounds possessing non-carcinogenic nature with comparatively high LD_{50} values. In vitro antimicrobial studies presented an enhanced activity for ligand in comparison their complexes against the microbial strains used in this study. *In vitro* anticancer studies by MTT assay of Fe-MHMMT complex disclosed a comparatively good anticancer action bearing an IC_{50} of 24 μM against breast cancer cells MCF7. *In vitro* antidiabetic studies by the α-amylase inhibitory method revealed a reasonably good antidiabetic activity for metal complexes. The conclusions arrived from molecular docking studies showing some significant binding of the compounds with selected targets are consistent with the in vitro anticancer and antidiabetic results. The significant biological activities showed by the studied compounds provide the scope for the *in vivo* studies to manifest the likelihood of these complexes' as anticancer agents for other cancer cell lines and antidiabetic agents.

Declarations

Author contribution statement

Abraham Joseph: Analyzed and interpreted the data; Wrote the paper.

Rugmini Ammal P: Conceived and designed the experiments; Performed the experiments.

Anupama R Prasad: Analyzed and interpreted the data; Contributed reagents, materials, analysis tools or data.

Funding statement

This research did not receive any specific grant from funding agencies in the public, commercial, or not-for-profit sectors.

Competing interest statement

The authors declare no conflict of interest.

Additional information

No additional information is available for this paper.

References

[1] O.A. El-Gammal, Mononuclear and binuclear complexes derived from hydrazine Schiff base NON donor ligand: synthesis, structure, theoretical and biological studies, Inorg. Chim. Acta. 435 (2015) 73–81.

[2] M.Reda. Abdel-Rahman, S.T.Mohamed. Makki, E.Tarik. Ali, Magdy A. Ibrahimb, 1,2,4-Triazine chemistry Part IV: synthesis and chemical behavior of 3-functionalized 5,6-Diphenyl-1,2,4-triazines towards some nucleophilic and electrophilic reagents, J. Heterocycl. Chem. 5 (52) (2015) 1595–1607.

[3] Pascal Dao, Daniel Lietha, Mélanie Etheve-Quelquejeu, Christiane Garbay, Huixiong Chen, Synthesis of novel 1,2,4-triazine scaffold as FAK inhibitors with antitumor activity, BioorganicMed. Chem. Lett. 27 (2017) 1727–1730.

[4] G.R. Priya Dharsini, C. Thanaraj, R. Velladurai, Metal chelates of tridentate (NNO) 1,2,4-triazine schiff base: synthesis, physico-chemical investigation and pharmacological screening, J. Inorg. Organomet. Polym. (Jan 1 2020) 1–8.

[5] K. Ramya, Abraham Joseph, Dependance of temperature on the corrosion protection properties of vanillin and its derivative HMATD, towards copper in nitric acid: theoretical and electroanalytical studies, Res. Chem. Intermed. 41 (2015) 1053–1077.

[6] C. Vidya Rani, M.P. Kesavan, S. Haseena, et al., Bidentate schiff base ligands appended metal(II) complexes as probes of DNA and plasma protein: in silico molecular modelling studies, Appl. Biochem. Biotechnol. (March 4 2020) 1–18.

[7] Dina A. Bakhotmah, Fatimah A. Alotaibi, Synthetic of some new fluorine compounds bearing 1, 2, 4-triazine moieties and the related hetero-polycyclic nitrogen systems as pharmacological probes-overview, Int. J. Org Chem. 10 (1) (2020) 17–38.

[8] K. Buldurun, N. Turan, E. Bursal, A. Mantarcı, F. Turkan, P. Taslimi, İ. Gülçin, Synthesis, spectroscopic properties, crystal structures, antioxidant activities and enzyme inhibition determination of Co (II) and Fe (II) complexes of Schiff base, Res. Chem. Intermed. 46 (1) (2020) 283–297.

[9] A. Kajal, S. Bala, S. Kamboj, N. Sharma, Saini, V "Schiff bases: a versatile pharmacophore, Journal of Catalysts (2013) 1–14, 2013.

[10] Kiran Singh, Sunita Raparia, Shashi Raparia, Synthesis, characterization and biological evaluation of triazine based Schiff base metal complexes, European Chemical Bulletin 5 (3) (2016) 92–98.

[11] A.I. Vogel, *A Text Book Of Quantitative Inorganic Analysis*", Longmann, Londom, 1975.

[12] A. Dornow, H. Mengel, P. Marx, Uber 1, 2, 4-triazine, I darstellung einiger neuer s-triazolo[3.2-c-]-as-triazine, Chem. Ber. 97 (1964) 2173–2178.

[13] Asif Husain, Aftab Ahmad, Shah Alam Khan, Mohd Asif Rubina Bhutani, Fahad A. Al-Abbasi, Synthesis, molecular properties, toxicity and biological evaluation of some new substituted imidazolidine derivatives in search of potent anti-inflammatory agents, Saudi Pharmaceut. J. 24 (2016) 104–114.

[14] T. Ozen, M. Taş, Screening and evaluation of antioxidant activity of some amido-carbonyl oxime derivatives and their radical scavenging activities, J. of Enz.Inh. and Med. Chem. 24 (2009) 1141–1147.

[15] Khaled Lotfy, Molecular modeling, docking and ADMET of dimethylthiohydantoin derivatives for prostate cancer treatment, J. Biophys. Chem. 6 (2015) 91.

[16] Rajesh Kumar Goel, Damanpreet Singh, Alexey Lagunin, Vladimir Poroikov, PASS-assisted exploration of new therapeutic potential of natural products, Med. Chem. Res. 20 (2011) 1509–1514.

[17] A.L. Barry, The Antimicrobial Susceptibility Test, Principles and Practices, fourth ed., E.L.B.S, 1976.

[18] J. Carmichael, W.G. DeGraff, A.F. Gazdar, J.D. Minna, J.B. Mitchell, Evaluation of a ttetrazolium based semiautomated colorimetric assay: assessment of radio sensitivity *Cancer*, Res. 47 (1987) 943–946.

[19] J.H. Sheikh, Iyo, M.T. Tsujiyama, I. MdAshabul, S.B. Rajat, A. Hitoshi, Total phenolic content, antioxidative, anti-amylase, anti-glucosidase, and antihistamine release activities of Bangladeshi fruits, Food Sci. Technol. Res. 14 (2008) 261–268.

[20] G.M. Morris, R. Huey, W. Lindstrom, M.F. Sanner, K. R Belew, D.S. Goodsell, A.J. Olson, AutoDock4 and AutoDockTools4: automated docking with selective receptor flexibility, J. Comput. Chem. 16 (2009) 2785–2791.

[21] http://accelrys.com/products/discovery-studio/visualization-download.php.

[22] K. Vanommeslaeghe, E. Hatcher, C. Acharya, S. Kundu, S. Zhong, J. Shim, E. Darian, O. Guvench, P. Lopes, I. Vorobyov, A.D. MacKerell Jr., et al., CHARMM general force field: a force field for drug-like molecules compatible with the CHARMM all-atom additive biological force fields, J. Comput. Chem. 31 (2010) 671–690.

[23] Garrett M. Morris, David S. Goodsell, Robert S. Halliday, William E. Hart Ruth Huey, Richard K. Belew, Arthur J. Olson, Automated docking using a Lamarckian genetic algorithm and an empirical binding free energy function, J. Comput. Chem. 19 (1998) 1639–1662.

[24] Kiran Singh, Sunita Raparia, Parveen Surain, Co (II), Ni (II), Cu (II) and Zn (II) Complexes of 4-(4-cyanobenzylideneamino)-3-mercapto-5-oxo-1, 2, 4-triazine: synthesis, characterization and biological studies, Med. Chem. Res. 24 (2015) 2336–2346.

[25] Kiran Singh Ritu Thakur, Vikas Kumar, Co (II), Ni (II), Cu (II), and Zn (II) complexes derived from 4-[{3-(4-bromophenyl)-1-phenyl-1H-pyrazol-4-ylmethylene}-amino]-3-mercapto-6-methyl-5-oxo-1, 2, 4-triazine, beni-suef university, J. Basic Appl. Sci. 5 (2016) 21–30.

[26] P Gurmit Singh, Ashutosh Singh, K Ashok Sen, Kiran Singh, Surendra N. Dubey, Ram N. Handa, Junghoon Choi, Synthesis and characterization of some bivalent metal complexes of schiff bases derived from as-triazine, Synth. React. Inorg. Met. Org. Chem. 32 (1) (2002) 171–187.

[27] C.N.R. Rao, R. Venkataraghavan, T.R. Kasturi, Contribution to the infrared spectra of organosulphur compounds, Can. J. Chem. 42 (1964) 36–42.

[28] Carlo Preti, Giuseppe Tosi, Tautomeric equilibrium study of thiazolidine-2-thione. Transition metal complexes of the deprotonated ligand, Can. J. Chem. 54 (10) (1976) 1558–1562.

[29] A.S. Ramasubramanian, B.R. Bhat, R. Dileep, S. Rani, Transition metal complexes of 5-bromosalicylidene-4-amino-3-mercapto-1, 2, 4-triazine-5-one: synthesis, characterization, catalytic and antibacterial studies", J. Serb. Chem. Soc. 76 (1) (2011) 75–83.

[30] Infrared and Raman Spectra of Inorganic and Coordination Compounds, Kazuo Nakamoto, Wiley Interscience Publication, 1997.

[31] A.B.P. Lever, Mantovanain, D.B.S. Ramaswamy, Infrared combination frequencies in coordination complexes containing nitrate groups in various coordination environments. A probe for the metal–nitrate interaction, Can. J. Chem. 49 (11) (1971) 1957–1964.

[32] D.C. Jicha, D.H. Busch, Complexes derived from strong field ligands. XIV. Heterometallic trinuclear complexes of β-mercaptoethylamine, Inorg. Chem. 1 (4) (1962) 878–883.

[33] H-Zh Ma, B. Wang, Q. Zh Shi, Synthesis and characterization of lanthanide (III) Schiff base complexes derived from cysteine and benzoin, Synth.react. inorg.met.org. chem 32 (3) (2002) 617–627.

[34] A.B. P Lever, Inorganic Electronic Spectroscopy, second ed., Elsiever, Amsterdam, 1984.

[35] P. Bindu, M.R.P. Kurup, Esr and electrochemical studies of four-and five-coordinate copper (II) complexes containing mixed ligands, Trans.Met.Chem 22 (1997) 578–582.

[36] L. Larabi, Y. Hared, A. Reguig, M. Mostafa, Synthesis, structural study and electrochemical properties of copper (II) complexes derived from benzene-and p-toluenesulphonylhydrazone, J. Serb. Chem. Soc. 68 (2) (2003) 85–96.

[37] S.F.A. Kettle, Coordination Compounds, ELBS, Essex, 1969.

[38] Sangamesh A. Patil, M. Manjunatha, D.Kulkarni Ajayakumar, Prema.S. Badami, Synthesis, characterization, fluorescence and biological studies of Mn(II), Fe(III) and Zn(II) complexes of Schiff bases derived from Isatin and 3-substituted-4-amino-5-mercapto-1,2,4-triazoles, Complex Metals 1 (1) (2014) 128–137.

[39] B.S. Garg, M.R.P. Kurup, S.K. Jain, Y.K. Bhoon, Synthesis and characterization of iron (III) complexes of a substituted 2-acetyi, pyridine thiosemicarbazone *synth*, React.Inorg.Met.Org.Chem. 28 (1998) 1415–1426.

[40] L. Calu, M. Badea, M.C. Chifiriuc, C. Bleotu, G. David, G. Ionit, L. Măruţescu, V. Lazăr, N. Stanică, I. Soponaru, D. Marinescu, R. Olar, Synthesis, spectral, thermal, magnetic and biological characterization of Co (II), Ni (II), Cu (II) and Zn (II) complexes with a Schiff base bearing a 1, 2, 4-triazole pharmacophore, J. Therm. Anal. Calorim. 120 (1) (2015) 375–386.

[41] A.B.P. Lever, The magnetic moments of some tetragonal nickel complexes, Inorg. Chem. 4 (5) (1965) 763–764.

[42] F.A. Cotton, G. Wilkinson, Advanced Inorganic Chemistry, Wiley Interscience Pub, New York, 1988.

[43] K. Singh, Y. Kumar, M.S. Barwa, Synthesis, characterization and thermal studies of Co(II), Ni(II), Cu(II) and Zn(II) complexes of some schiff bases derived from 4-Amino-3-mercapto-6-methyl-5-oxo-1,2,4 triazine *S*, Afr.J.Chem. 63 (2010) 169–174.

[44] Preeti Jain, Vandna Singh, Sabir Ali, Vishwas Tripathi, Upendra Saraswat, Synthesis, characterization, molecular docking and biological activity of 5, 6-bis-(4-fluoro-phenyl)-3, 4, 7, 8-tetraaza-bicyclo [8.3. 1] tetradeca-1 (13), 4, 6, 10 (14), 11-pentaene-2, 9-dione and its transition metal complexes, Journal of Saudi Chemical Society 22 (5) (2018) 546–557.

[45] B.J. Hathaway, D. E, Billing. "The electronic properties and stereochemistry of mono-nuclear complexes of the copper (II) ion, Coord. Chem. Rev. 5 (2) (1970) 143–207.

[46] Abd-Elzaher, M. Mokhles, et al., Synthesis, anticancer activity and molecular docking study of Schiff base complexes containing thiazole moiety, Beni-Suef University Journal of Basic and Applied Sciences 5 (1) (2016) 85–96.

[47] A. Verma, Lead finding from phyllanthusdebelis with hepatoprotective potentials, Asi. Pac. J. Trop. Biomed. 1 (2012) 735–737.

[48] Dhanaraj, Chellaian Justin, Jijo Johnson, Studies on some metal complexes of quinoxaline based unsymmetric ligand: synthesis, spectral characterization, in vitro biological and molecular modeling studies, J. Photochem. Photobiol. B Biol. 161 (2016) 108–121.

[49] Tahmeena Khan1,2, Shalini Dixit3, Rumana Ahmad4, Saman Raza2, Azad1 Iqbal, Seema Joshi2, Abdul Rahman Khan, Molecular docking, PASS analysis, bioactivity score prediction, synthesis, characterization and biological activity evaluation of a functionalized 2-butanone thiosemicarbazone ligand and its complexes, Journal of chemical biology 10 (3) (2017) 91–104.

[50] C.A. Lipinski, F. Lombardo, B.W. Dominy, P.J. Feeney, Experimental and computational approaches to estimate solubility and permeability in drug discovery and development settings, Adv. Drug Deliv. Rev. 46 (2001) 3–26.

[51] C.J. Dhanaraj, J. Johnson, DNA interaction, antioxidant and in vitro cytotoxic activities of some mononuclear metal(II) complexes of a bishydrazone ligand, Mater. Sci. Eng. C 78 (2017) 1006–1015.

[52] Bradley C. Doak, Kihlberg Jan, How beyond rule of 5 drugs and clinical candidates bind to their targets, J. Med. Chem. 59 (6) (2016) 2312–2327.
[53] Feixiong Cheng, Weihua Li, Yadi Zhou, Jie Shen, Zengrui Wu, Guixia Liu, Philip W. Lee, Yun Tang, admetSAR: a comprehensive source and free tool for assessment of chemical ADMET properties, J. Chem. Inf. Model. 52 (2012) 3099–3105.
[54] N. Quignot, J. Hamon, F. Bois, Extrapolating in vitro results to predict human toxicity, in: A. Bal-Price, P. Jennings (Eds.), Vitro Toxicology Systems, Methods in Pharmacology and Toxicology Series, Springer Science, New York, USA, 2014, pp. 531–550.
[55] Jong Hwan Sung, Mandy B. Esch, Michael L. Shuler, Integration of in silico and in vitro platforms for pharmacokinetic–pharmacodynamic modeling, Expert opin drug metab. toxicol 6 (9) (2010) 1063–1081.
[56] M. Salehi, A. Amoozadeh, A. Salamatmanesh, M. Kubicki, G. Dutkiewicz, S. Samiee, A. Khaleghian, Synthesis, characterization, crystal structures, computational studies, and antibacterial activities of two new Schiff bases derived from isophthalaldehyde, J. Mol. Struct. 1091 (2015) 81–87.
[57] Anthony J. Turner, Natalia N. Nalivaeva, Peptide degradation (Neprilysin and other regulatory peptidases), in: Handbook of Biologically Active Peptides, Academic Press, 2013, pp. 1757–1764.
[58] S.R. Pattan, S.B. Pawar, S.S. Vetal, U.D. Gharate, S.B. Bhawar, The scope of metal complexes in drug design - a review, Indian Drugs 49 (11) (2012) 5–12.
[59] Hroob Al, M. Amir, et al., Ginger alleviates hyperglycemia-induced oxidative stress, inflammation and apoptosis and protects rats against diabetic nephropathy, Biomed. Pharmacother. 106 (2018) 381–389.
[60] E.A. Ostrakhovitch, M.G. Cherian, Differential regulation of signal transduction pathways in wild type and mutated p53 breast cancer epithelial cells by copper and zinc, Arch. Biochem. Biophys. 423 (2) (2004) 351–361.
[61] E. Sneha Jose, Jessica Elizabeth Philip, A.A. Shanty, M.R.P. Kurup, P.V. Mohanan, Novel class of mononuclear 2-methoxy-4-chromanones ligated Cu (II), Zn (II), Ni (II) complexes: synthesis, characterisation and biological studies, Inorg. Chim. Acta. 478 (2018) 155–165.
[62] Sundaramurthy Lakshmi, Santha, et al., Synthesis, crystal structures, spectroscopic characterization and in vitro antidiabetic studies of new Schiff base Copper (II) complexes, J. Chem. Sci. 128 (7) (2016) 1095–1102.
[63] G.M. Morris, R. Huey, W. Lindstrom, M.F. Sanner, R.K. Belew, D.S. Goodsell, A.J. Olson, AutoDock4 and AutoDockTools4: automated docking with selective receptor flexibility, J. Comput. Chem. 30 (1) (2009) 2785–2791.
[64] S.V.G. Reddy, K. Thammi Reddy, V. Valli Kumari, Syed Hussain Basha, Molecular docking and dynamic simulation studies evidenced plausible immunotherapeutic anticancer property by Withaferin A targeting indoleamine 2,3-dioxygenase, J. Biomol. Struct. Dyn. 33 (12) (2015) 2695–2709.
[65] Sreenivasa reddy, Syed Hussain Basha, Bethapudi Prakash, Majji Rambabu, A.,N.V.S. Firoz, M. Viswanadha murty, Anti-angiogenesis property by Quercetin compound targeting VEGFR2 elucidated in a computational approach", Eur. J. of Biotech. and Biosci. 2 (6) (2014) 30–46.